Journal of Biomolecular NMR, **21:** 289–306, 2001.
KLUWER/ESCOM

^{1}H-^{1}H correlations across N–H•••N hydrogen bonds in nucleic acids

Ananya Majumdar*, Yuying Gosser & Dinshaw J. Patel
Cellular Biochemistry and Biophysics Department, Memorial Sloan-Kettering Cancer Center, 1275 York Avenue, New York 10021, U.S.A.

Received 4 May 2001; Accepted 27 August 2001

Key words: hydrogen bond, $^{2h}J_{NN}$, HNN-COSY, H2(N1N3)H3, H5(N3N1)H1, H6(N3N1)H1, H_2(N2N7)H8

Abstract

In $^{2H}J_{NN}$-COSY experiments, which correlate protons with donor/acceptor nitrogens across N_d•••HN_a bonds, the receptor nitrogen needs to be assigned in order to unambiguously identify the hydrogen bond. For many situations this is a non-trivial task which is further complicated by poor dispersion of (N_a,N_d) resonances. To address these problems, we present pulse sequences to obtain direct, internucleotide correlations between protons in uniformly ^{13}C/^{15}N labeled nucleic acids containing N_d•••HN_a hydrogen bonds. Specifically, the pulse sequence H2(N1N3)H3 correlates H2(A,ω_1):H3(U,ω_2) protons across Watson–Crick A–U and mismatched G•A base pairs, the sequences H5(N3N1)H1/H6(N3N1)H1 correlate H5(C,ω_1)/H6(C,ω_1):H1(G,ω_2) protons across Watson–Crick G-C base pairs, and the H_2(N2N7)H8 sequence correlates NH_2(G,A,C;ω_1):H8(G,A;ω_2) protons across G•G, A•A, sheared G•A and other mismatch pairs. These ^{1}H-^{1}H connectivities circumvent the need for independent assignment of the donor/acceptor nitrogen and related degeneracy issues associated with poorly dispersed nitrogen resonances. The methodology is demonstrated on uniformly ^{13}C/^{15}N labeled samples of (a) an RNA regulatory element involving the HIV-1 TAR RNA fragment, (b) a multi-stranded DNA architecture involving a G•(C-A) triad-containing G-quadruplex and (c) a peptide-RNA complex involving an evolved peptide bound to the HIV-1 Rev response element (RRE) RNA fragment.

Introduction

Ever since the discovery of *trans*-hydrogen bond $^{2h}J_{NN}$ coupling constants in nucleic acids (Dingley and Grzesiek, 1998; Pervushin et al., 1998) a number of $^{2h}J_{NN}$ and $^{4h}J_{NN}$ correlated spectroscopic techniques have been developed (Majumdar et al., 1999a,b; Liu et al., 2000a; Dingley et al., 2000; Hennig and Williamson, 2000; Luy and Marino, 2000; Majumdar et al., 2001) and applied to structural, dynamical and physico-chemical studies of a variety of RNA (Wöhnert et al., 1999a; Jiang et al., 1999; Hennig and Williamson, 2000; Luy and Marino, 2000; Gosser et al., 2001) and DNA (Dingley et al., 1999; Kettani et al., 1999, 2000a,b; Kojima et al., 2001; al-Hashimi et al., 2001a, Barfield et al., 2001) systems and their complexes (Liu et al., 2000b; al-Hashimi et al., 2001b) (reviews summarizing some of these developments may be found in Gemmeker, 2000; Mollova and Pardi, 2000; Dingley et al., 2001, Grzesiek et al., 2001, Zidek et al., 2001). Some of the methodology has been aimed at overcoming technical difficulties such as large chemical shift differences between donor and acceptor nitrogens (Majumdar et al., 1999a; Dingley et al., 2000) whereas others have dealt with circumventing problems related to exchange broadening of the hydrogen bonded proton (Majumdar et al., 1999b, 2001; Hennig and Williamson, 2000; Luy and Marino, 2000). One-dimensional $^{2h}J_{NN}$ spectroscopy with selective ^{15}N labeling and direct ^{15}N detection has also been employed (Kojima et al., 2000). The basic objective of two-dimensional experiments has been to generate a ^{1}H-^{15}N correlation spectrum in which a proton on the donor/acceptor base shows a cross peak to the acceptor/donor nitrogen involved in the N_d–H•••N_a

*To whom correspondence should be addressed. E-mail: majumdar@sbnmr1.mskcc.org

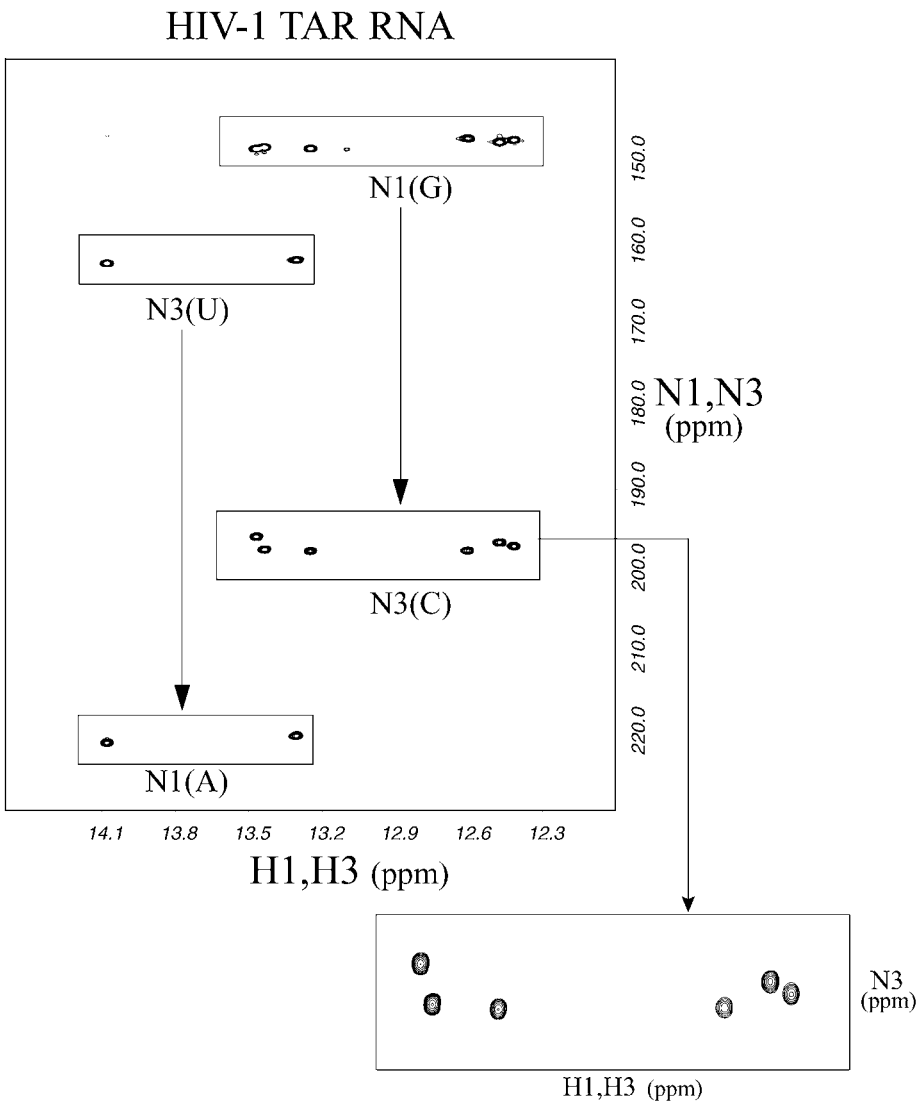

Figure 1. HNN-COSY spectrum of the uniformly $^{13}C/^{15}N$ labeled fragment derived from HIV-1 TAR RNA (Figure 2a), showing cross peaks between hydrogen bonded protons to their respective donor and acceptor nitrogens within A–U and G–C Watson–Crick base pairs. Uridine H3 protons show cross peaks to N3(U) and N1(A) nitrogens, whereas guanine H1 protons show cross peaks to N1(G) and N3(C). The H1(G):N3(C) region is expanded to highlight the degree of degeneracy amongst N3(C) nitrogens. The spectrum was acquired with 32 transients, 1024 t_2 and 250 t_1 complex data points and spectral widths of 14.0 (ω_2) and 6.1 (ω_1) kHz, ($t_2^{max} = 71.0$ ms, $t_1^{max} = 41$ ms). A relaxation delay of 1.5 s was used, resulting in total data acquisition time of $\sim$7 h.

hydrogen bond. In the HNN-COSY and soft-HNN COSY experiments, the hydrogen bonded proton is correlated with the acceptor nitrogen. In the event of exchange broadening of the hydrogen bonded proton, a non-exchangeable proton on the acceptor base is correlated with the donor nitrogen in the H(CN)N(H) type of experiments (Majumdar et al., 1999b; Hennig and Williamson, 2000; Luy and Marino, 2000), or a proton on the donor base is correlated with the acceptor nitrogen in the H2N3N1 and (N)H6N3H2 sequences for detecting sheared G•A mismatches (Majumdar et al., 2001).

Useful as these experiments are, there are two immediate consequences of recording $^{2h}J_{NN}$ correlated spectra in this fashion: (a) the donor/acceptor nitrogen needs to be assigned. This is an important issue especially when the folding topology of the nucleic acid is either unknown or not known accurately, and necessi-

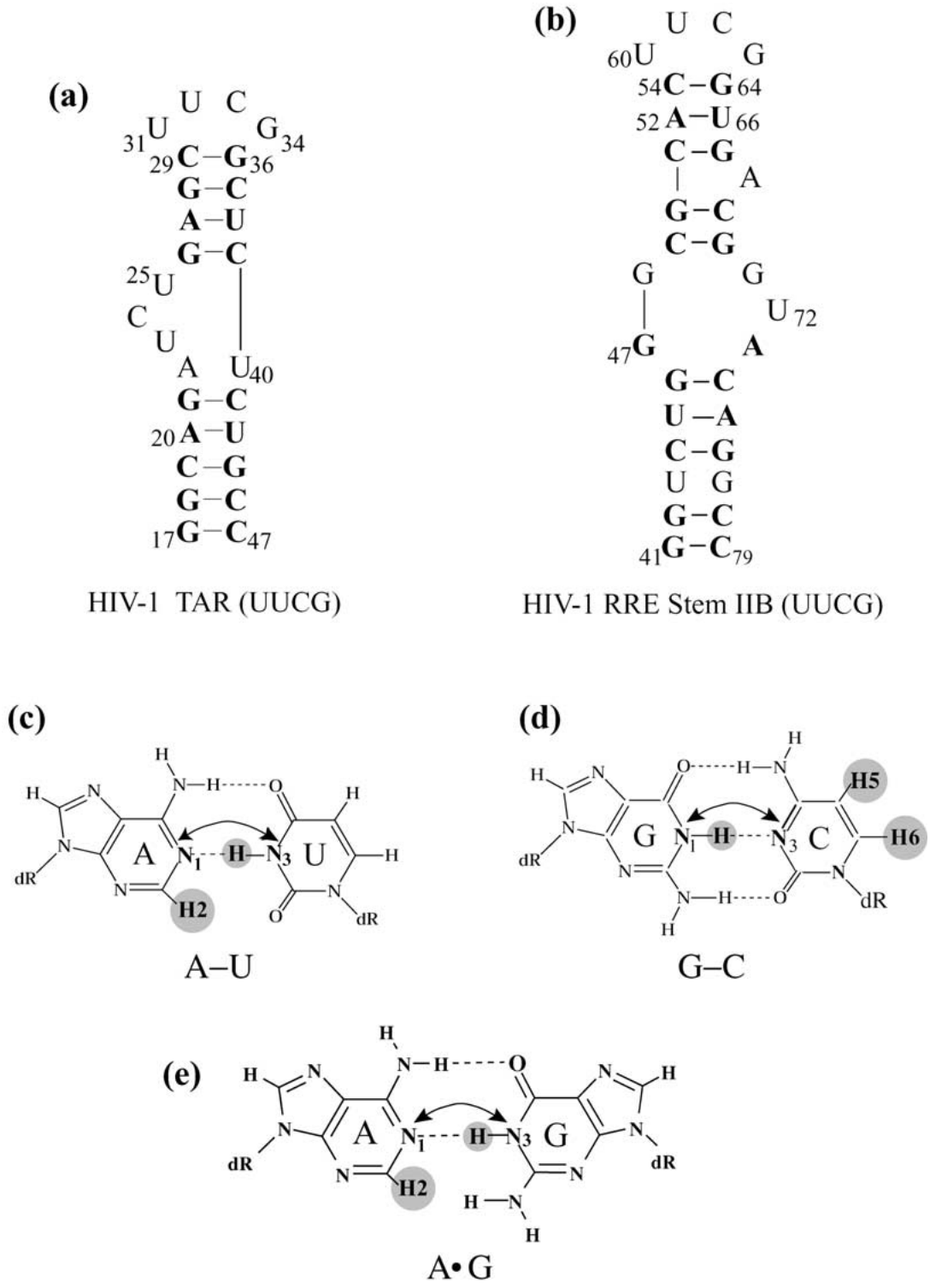

Figure 2. Primary sequences and RNA folding topologies: (a) the RNA regulatory element involving the HIV-1 TAR RNA fragment containing a stable UUCG hairpin loop replacing the natural CUGGGA hairpin, and (b) an RNA regulatory element involving the evolved peptide bound to the HIV-1 Rev response element (RRE) RNA stem II-B. The Watson–Crick (c) A–U and (d) G–C base pairs, and the (e) A•G mismatch are also shown, indicating the ^{1}H-^{1}H correlations (gray circles) described in this paper and the relevant $^{2h}J_{NN}$ couplings (arrows).

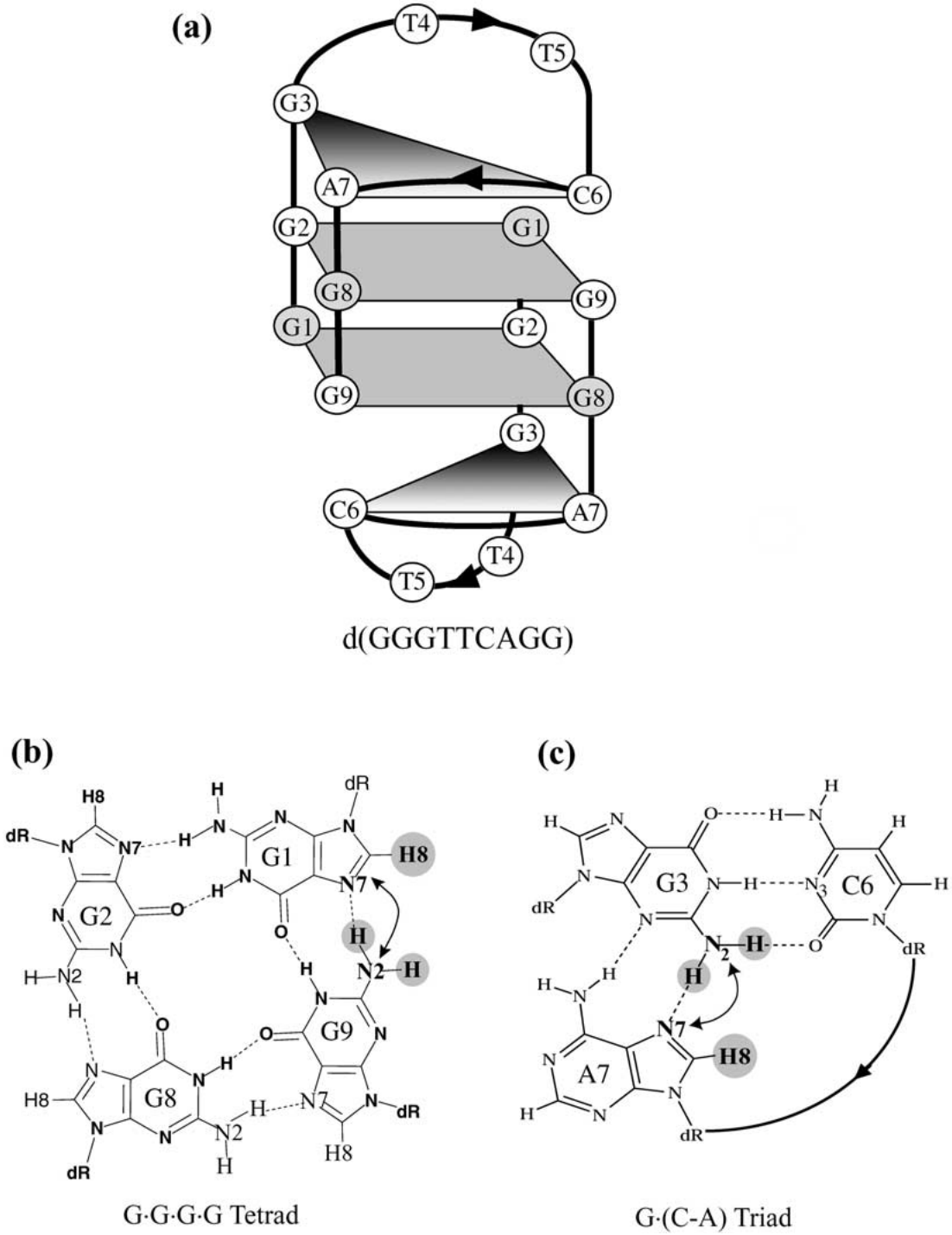

Figure 3. (a) Schematic of the multi-stranded DNA architecture involving a dimeric G•(C-A) triad-containing G-quadruplex formed by d(GGGTTCAGG) in Na cation solution. The (b) G•G•G•G tetrad and the (c) G•(C-A) triad are also shown schematically, indicating the ^{1}H-^{1}H correlations (gray circles) described in this paper and the relevant $^{2h}J_{NN}$ couplings (arrows).

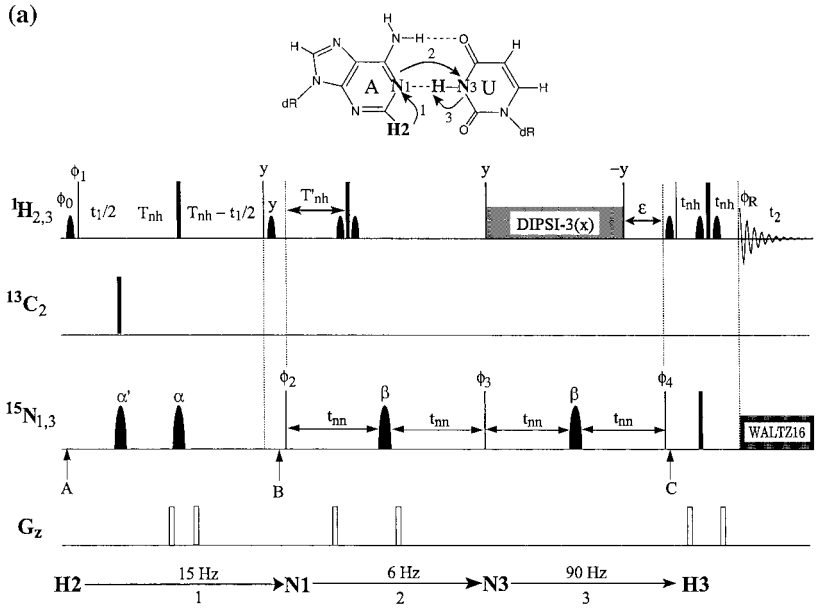

Figure 4. Pulse sequences and schematic description of magnetization transfer pathways in the *trans*-hydrogen bond ^{1}H-^{1}H correlation experiments (a) H2(N1N3)H3 in an A–U Watson–Crick and mismatch AG base pair, (b,c) H5(N3N1)H1, H6(N3N1)H1 in a Watson–Crick G–C pair and (d) H_2(N2N7)H8 in a mismatch G•G and sheared G•A pair. The basic elements of the magnetization transfer pathway is outlined below each sequence, and also indicated on the schematic of the appropriate base pair, above the sequence. The appropriate coupling constant and step number are shown above and below, respectively, of each arrow marker in the transfer pathway outline below the pulse sequence. Narrow and thick lines represent high power 90° and 180° pulses, respectively, applied with phase x unless explicitly specified. High power pulses were applied with rf field strengths of 45 kHz (^{1}H), 18.5 kHz (^{13}C) and 6.6 kHz (^{15}N). All water-flipback (Grzesiek and Bax, 1993) and WATERGATE (Piotto et al., 1992) pulses on ^{1}H were applied as 1.8 ms rectangular pulses with phase −x, unless explicitly specified. The ^{1}H carrier was placed at 4.75 ppm for (a)–(c), and at 5.0 ppm for (d). All z-gradients were rectangular, applied for 0.5 ms at approximately 15 G/cm. ^{1}H decoupling was applied using a DIPSI-3 sequence (Shaka et al., 1988) employing an rf field strength of 8 kHz. ^{15}N WALTZ16 decoupling (Shaka et al., 1983) during acquisition was performed using 1–1.3 kHz rf fields. Quadrature detection along ω_1 was achieved via States-TPPI phase cycling (Marion et al., 1989) of $\phi_0(-x)$ and $\phi_1(x)$ in (a) and (d), and ϕ_1 (x),ϕ_2 (y) and ϕ_3 (−x) in (b, c). Details of sequence-specific pulse-widths, delays and phase-cycles are: (a) *H2(N1N3)H3.* The ^{13}C carrier was placed at 155 pm (δ_{C2}). The ^{15}N carrier was initially placed at 220 ppm (δ_{N1} of adenine, point A) until point B when it was moved to 182.5 ppm (center of uridine δ_{N3} and adenine δ_{N1}) and at point C it was moved to 162 ppm (uridine δ_{N3}). The shaped pulse labeled α was a 2.5 ms G3 pulse (Emsley and Bodenhausen, 1990) and the pulse labeled β was a 2.78 ms G3 pulse centered at 182.5 ppm and cosine modulated to achieve simultaneous inversion at 220 and 162 ppm. The pulse labeled α′ was a 216 μs rectangular pulse, phase modulated at −65 ppm to achieve selective inversion at δ_{N3}(U)/δ_{N1}(G) with minimal excitation at δ_{N1}(A). Delays used were: T_{nh}: 13.0 ms, T'_{nh}: 11.0 ms, t_{nn}: 22.0 ms, ε: 5.5 ms, t_{nh}: 2.5 ms. Phase-cycles: ϕ_0,ϕ_1 see above; ϕ_2 = x, −x, ϕ_3 = x, x,−x, −x, ϕ_4 = 4(x), 4(−x), ϕ_R = 2(x,−x),2(−x,x). (b). *H5(N3N1)H1.* The ^{13}C carrier was initially placed at 100 ppm (δ_{C5}, point A) and moved to 167 ppm (δ_{C4}) at point D. Selective pulses: α: 1.95 ms G3 pulse, cosine modulated for simultaneous excitation at 100 and 167 ppm, β: 1.0 ms time-reversed qsneeze, β′: 1.0 ms qsneeze pulse, δ: 1.5 ms G3 pulse, γ: 0.5 ms frequency-shifted G3 pulse with inversion at 100 ppm (δ_{C5}), η: 3.0 ms G3 pulse. The ^{15}N carrier was initially positioned at 198 ppm (δ_{N3} of cytosine) until point E, when it was moved to 173 ppm (center of δ_{N3}:C and δ_{N1}:G) and to 148 ppm (δ_{N1} of guanine) at point F. Selective pulses: δ′: 1.0m G3 pulse, χ: 3.75 ms G3 pulse cosine modulated for simultaneous excitation at 148 and 198 ppm. Delays: t_{ch}: 1.2 ms, t_{cc}: 4.0 ms, t_{cn}: 18 ms for the TAR fragment (Figures 6a and 6b) and 13 ms for the peptide–RRE complex (Figures 9a and 9b), t_{nn}: 24 and 20 ms, for the TAR RNA and peptide–RRE complex, respectively, ε: 5.5 ms, t_{nh}: 2.5 ms. Phase cycles: ϕ_1, ϕ_2, ϕ_3 see above; ϕ_4 = x,−x, ϕ_5 = x, x, −x, -x, ϕ_6 = 4(x), 4(−x), ϕ_R = x, −x, −x, x. *H6(N3N1)H1.* Identical to the H5(N3N1)H1 sequence except that the ^{13}C carrier was initially placed (point A) at 140 ppm (δ_{C6}) and the sequence between points B and C replaced with the one in (c). At point b – prior to the ^{13}C DIPSI-3 (Shaka et al., 1988) sequence – the ^{13}C carrier was moved to 120 ppm (center of δ_{C5} and δ_{C6}), and to 100 ppm (δ_{C5}) at point b′. The duration of the DIPSI-3 sequence was 7.4 ms, using an RF field strength of 8.1 kHz. (c). *H_2(N2N7)H8.* The ^{15}N carrier was initially placed at 85 ppm (δ_{N2}, point A) until point B, when it was moved to 235 ppm (δ_{N7}). Selective pulses: α: 2.0 ms G3 pulse, β: 1.2 ms time-reversed qsneeze pulse, β′: 1.2 ms qsneeze pulse, γ, γ′: 1.0 ms G3 pulses with off-resonance excitation at 235 ppm (150 ppm phase-modulation) and 85 ppm (−150 ppm phase modulation) respectively and compensated for Bloch-Siegert type effects (Vuister and Bax, 1992). Delays: t_{nh}: 2.5 ms, ε: 2.75 ms, t_{nn}: 24 ms, T_{nh}: 15 ms. ^{13}C WALTZ-16 decoupling (4 kHz rf field strength) was also applied during acquisition. Phase cycles: ϕ_0, ϕ_1 see above; ϕ_4 = x, −x, ϕ_5 = x, x, −x, −x, ϕ_6 = 4(x), 4(−x), ϕ_R = x, −x, −x, x, −x, x, x, −x.

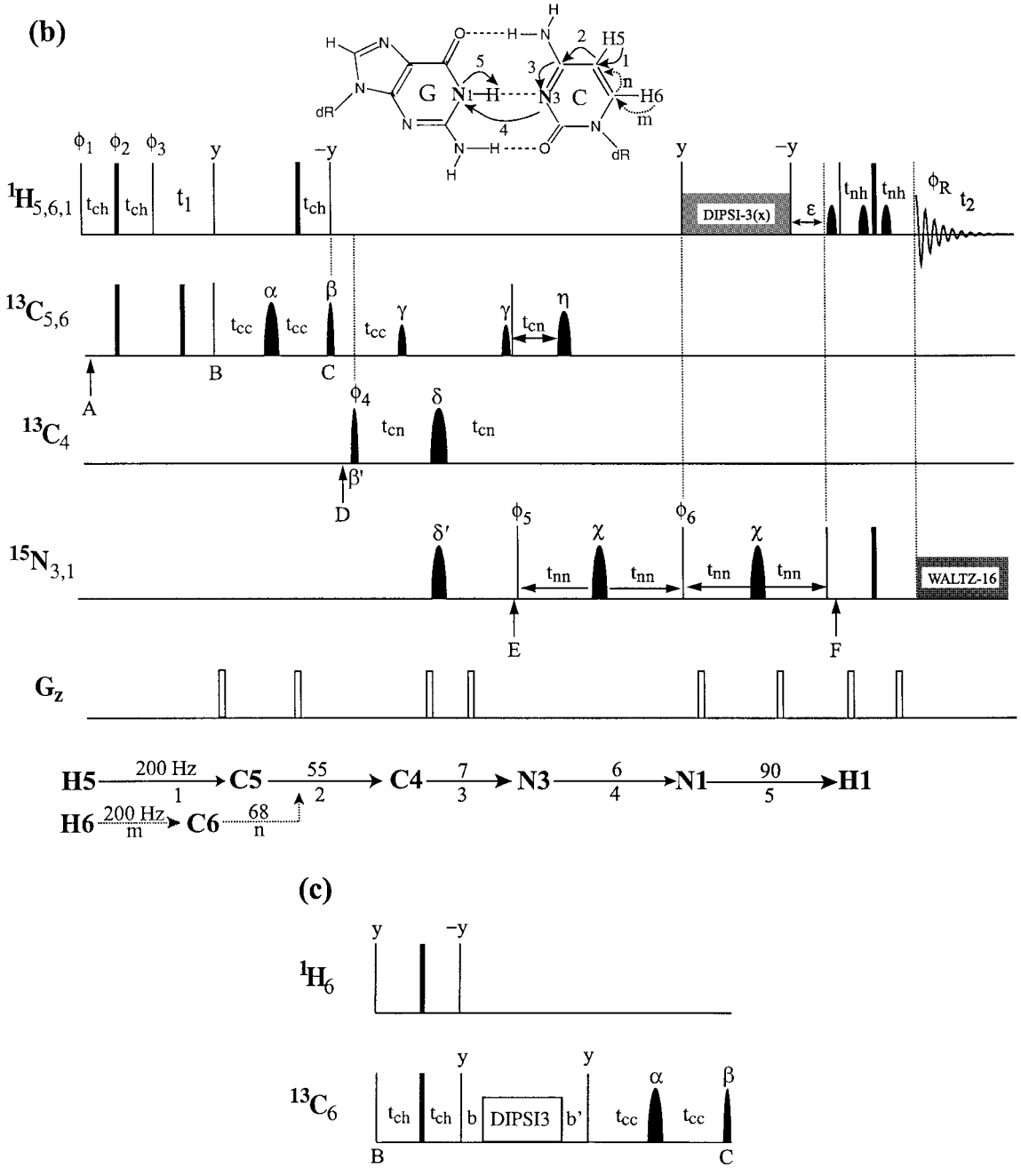

Figure 4. Continued.

tates the development of a parallel set of experiments for correlating the donor/acceptor nitrogen with other, independently assigned protons. In this process, one encounters the second problem, namely, (b) degeneracy among the nitrogens that need to be assigned. In nucleic acids, the dispersion of hydrogen bonded ^{15}N nuclei is often poor. This is illustrated in the HNN-COSY spectrum (Figure 1) of a uniformly $^{13}C/^{15}N$ labeled 27 nucleotide RNA regulatory element involving the HIV-1 TAR RNA, containing a stable UUCG hairpin loop replacing the natural CUGGGA hairpin loop (Figure 2a). Excluding the terminal G–C pair for which the imino proton is considerably exchange broadened, the guanine imino (H1) protons show cross

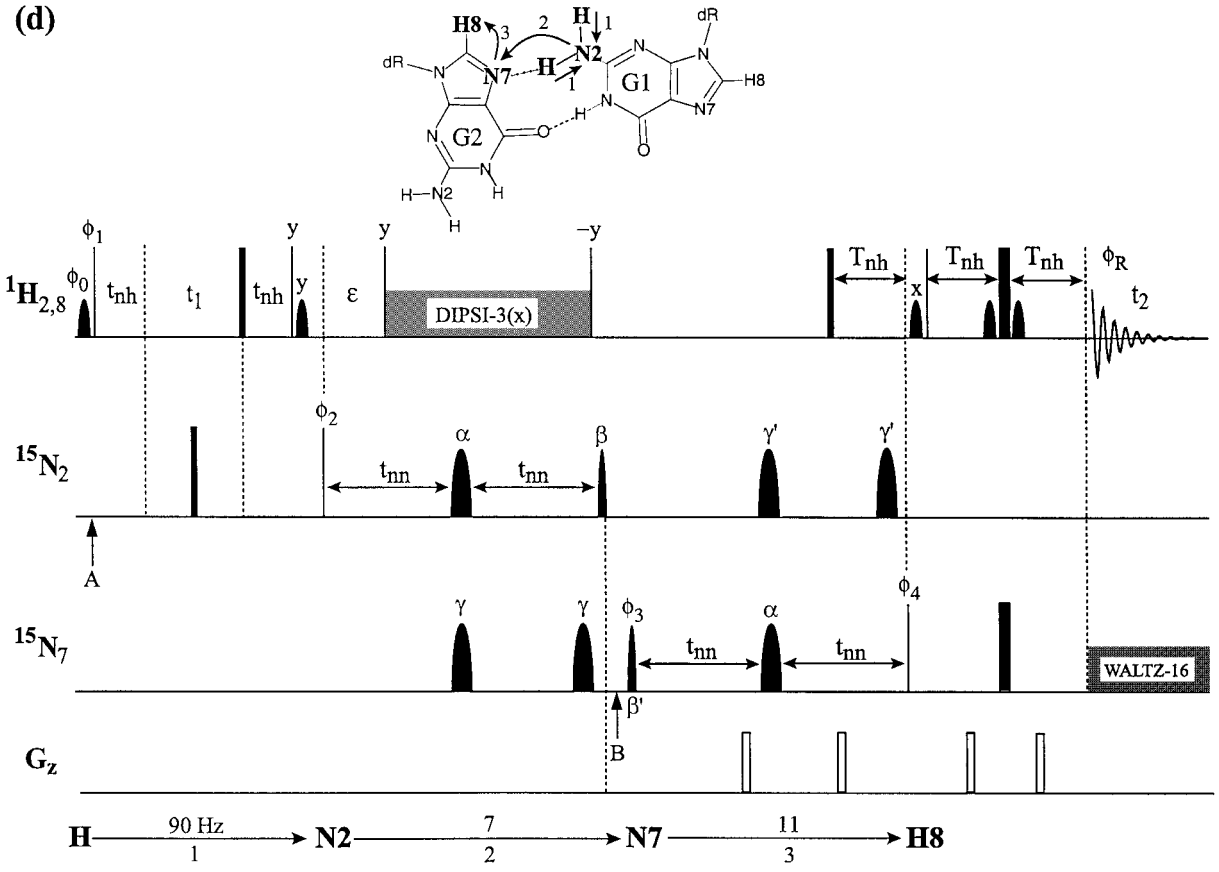

Figure 4. Continued.

peaks to the directly bonded donor guanine N1 nitrogen as well as the acceptor cytosine N3 nitrogen, mediated through the trans-H-bond $^{2h}J_{NN}$ coupling. While the identities of the donor N1 nitrogens of the guanines may be obtained from independent H1 proton assignments, the corresponding acceptor N3 nitrogens of the cytosines need to be assigned separately. This is usually achieved through N4H4$_{1,2}$(amino):N3 (Rudisser et al., 1999) or H5:N3 COSY (Gosser et al., 2001) spectra of cytosines. However, it is evident from the expansion of the H1(G):N3(C) cross peak region in Figure 1 (lower right), that considerable degeneracy exists within the N3 nitrogen frequencies, preventing the assignment procedure from being straightforward.

In A–U base pairs the imino (H3) resonances of uridines show cross peaks to the directly bonded N3 (uridine) and *trans*-hydrogen-bond N1 (adenine) resonances. As in the case of G–C pairs, the donor uridine N3 nitrogens are identifiable from H3 proton assignments, but the acceptor adenine N1 nitrogens need to assigned either from additional long range H2-N1 HSQC spectra or NOE cross peaks between H3 and H2 protons. Since the TAR RNA fragment has only two stable A–U pairs, with resolved N1 nitrogens, degeneracy is not an issue. However, it would still be desirable to obtain *direct* correlations between the H3(U) and H2(A) protons so that the intermediate N1(A) assignment step can be eliminated. Furthermore, A–U rich systems will undoubtedly suffer from degeneracy problems within the N1(A) nitrogens, in a manner analogous to the G–C pairs in TAR RNA.

Although we have highlighted these problems in the context of Watson–Crick base pairs, they are actually far more general in nature, and equally applicable to mismatched base pairs containing N-H$_n$•••N (n = 1,2) hydrogen bonds, such as in G•G, G•A, A•A alignments, observed frequently in RNA and higher order DNA structures (reviewed in Hermann and Westhof 1999; Patel et al., 1999; Masquida and Westhof, 2000; Westhof and Fritsch, 2000).

The solution to the problem lies in recognizing that it is *not necessary* to correlate protons specif-

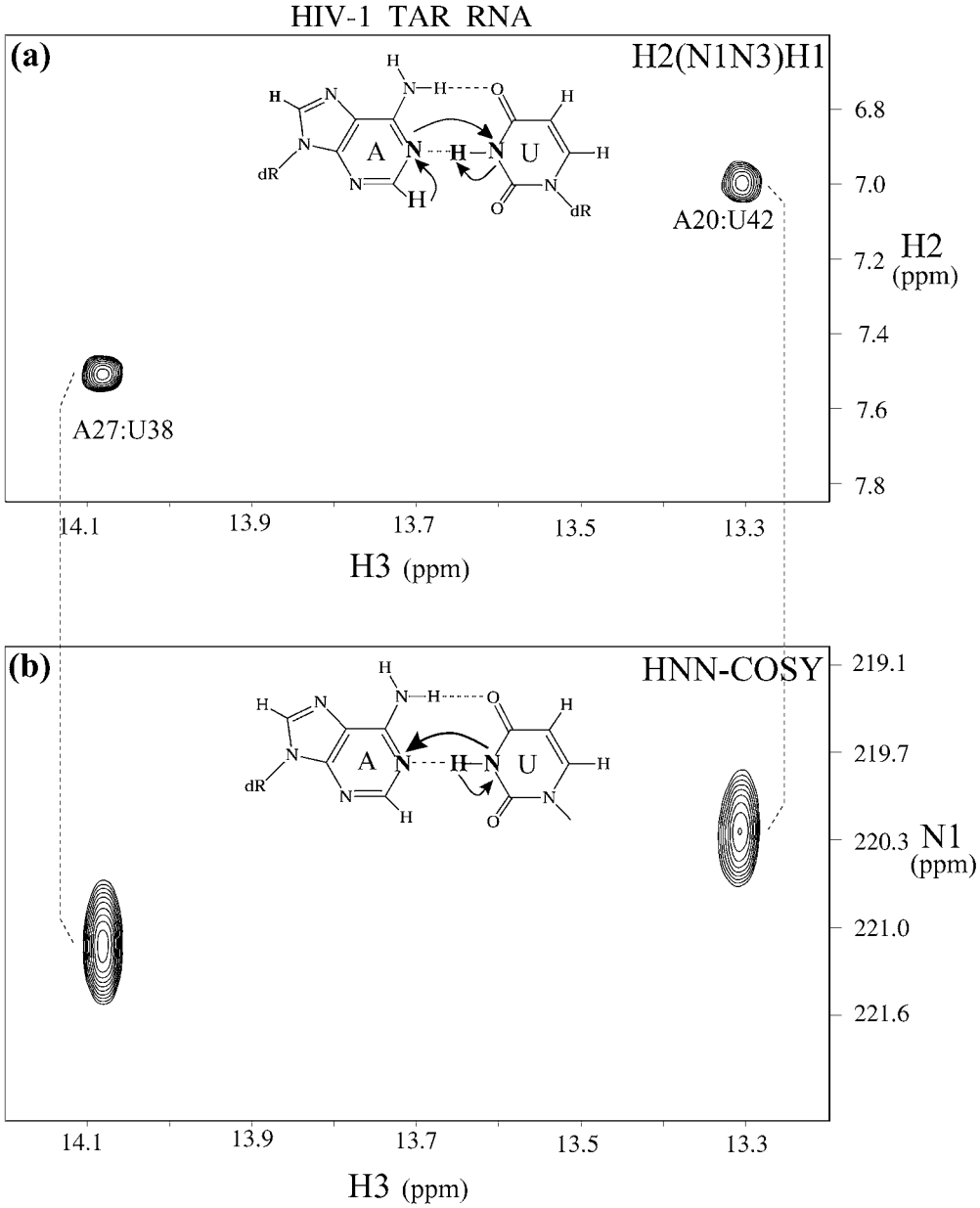

Figure 5. Regions of H2(N1N3)H3 (a) and HNN-COSY (b) spectra of the uniformly $^{13}C/^{15}N$ labeled fragment of the HIV TAR RNA, showing cross peaks between H3 protons of uridine and (a) H2 protons and (b) N1 nitrogens of adenine, in the two Watson–Crick A–U base pairs (see Figure 1). The H2(N1N3)H3 spectrum was acquired with 16 transients, 1024 t_2 and 38 t_1 complex data points and spectral widths of 14.0 (ω_2) and 1.5 (ω_1) kHz, ($t_2^{max} = 73$ ms, $t_1^{max} = 25$ ms). A relaxation delay of 1.5 s was used, resulting in total data acquisition time of $\sim$35 minutes. The spectrum was folded in the ω_1 dimension. Acquisition parameters for the HNN-COSY spectrum are given in the legend to Figure 1.

ically with trans-hydrogen bond nitrogens. Hydrogen bonding between two bases is established if we can correlate *any two* nuclei on the acceptor and donor bases via the $^{2h}J_{NN}$ bridge. In this paper, we have adopted the view that since protons need to be assigned *anyway*, for structure determination purposes, a good choice would be to try and correlate *protons* residing on the paired nucleotides, via the $^{2h}J_{NN}$ couplings. This not only eliminates the need for assigning the nitrogens separately, but also, by providing information complementary to the HNN-COSY experiment, helps resolve degeneracy is-

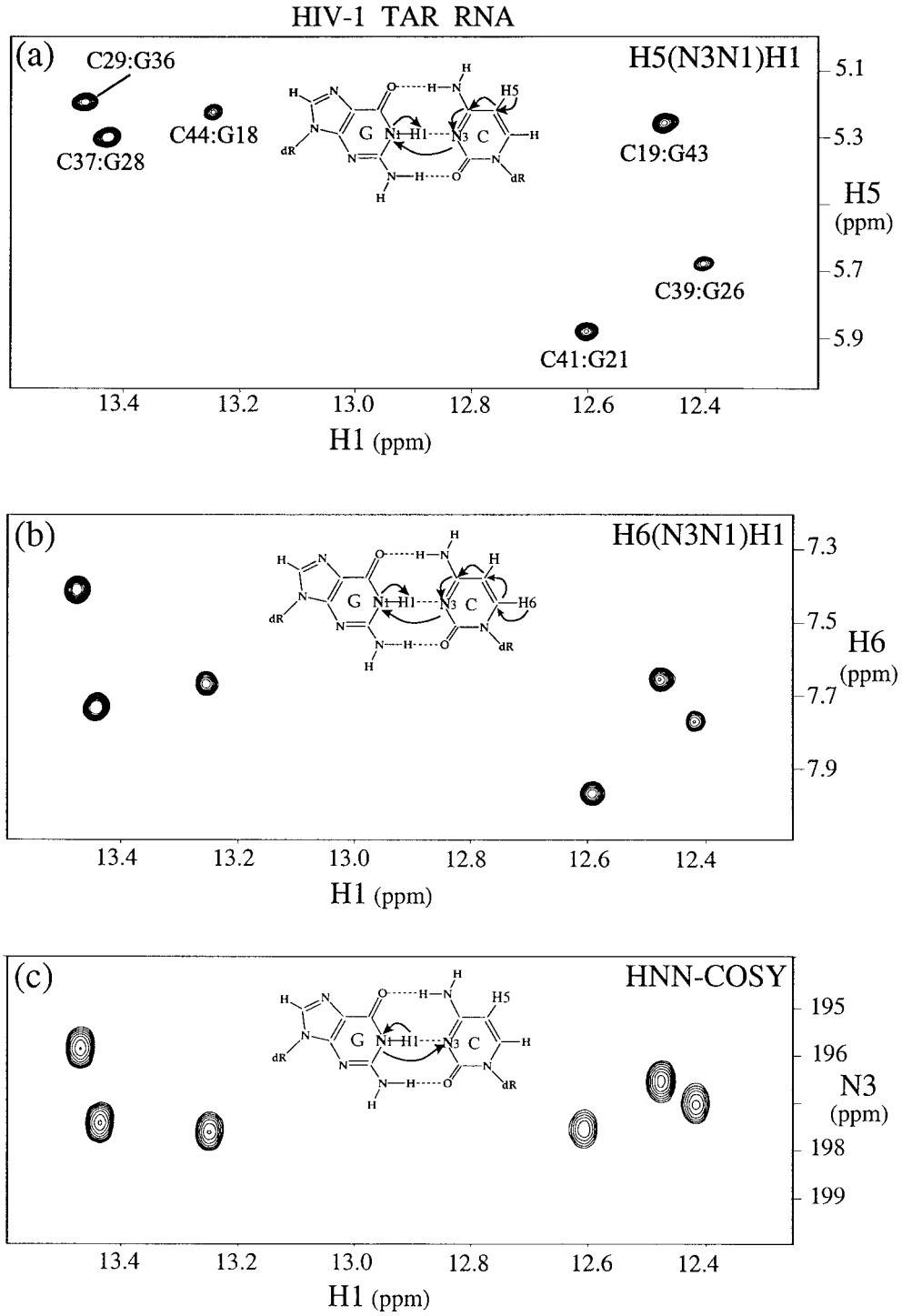

Figure 6. Regions of the (a) H5(N3N1)H1, (b) H6(N3N1)H1 and (c) HNN-COSY spectra of the uniformly $^{13}C/^{15}N$ labeled fragment of the HIV TAR RNA, showing cross peaks between H1 protons of guanine and (a) H5 and, (b) H6 protons, and (c) N3 nitrogens of cytosine, in six of the seven Watson–Crick G–C base pairs (see Figure 1). Spectra were acquired with (a) 64 and (b) 96 transients, 896 complex t_2 data points, a spectral width of 12.5 kHz along $\omega_2(t_2^{max} = 72$ ms), and a relaxation delay of 1.3 s. Parameters for the indirect dimension were: complex data points: (a) 75, (b) 74; spectral width (kHz): (a) 1.5, (b) 1.8; t_1^{max} (ms): (a) 49.0, (b) 41.0; total data acquisition time (h): (a) 4.2, (b) 6.2. Adequate S/N was achieved in about half the total acquisition time. Spectra were folded in the ω_1 dimension. Parameters for the HNN-COSY spectrum are provided in the legend to Figure 1.

sues associated with the poorly dispersed nitrogen nuclei. In this work, we present pulse sequences – which can be generally classified as H(NN)H and H(CNN)H – to establish the following kinds of ^{1}H-^{1}H connectivities mediated through hydrogen bonds: (a) H2(adenine)–H3(thymine/uridine) in A–T/U base pairs, (b) H5,H6(cytosine)–H1(guanine) correlations in G–C Watson–Crick base pairs and (c) NH_2(guanine/adenine)-H8(guanine/adenine) correlations in G•G, G•A and A•A mismatches, where either the Watson–Crick edge or the minor groove of the donor nucleotide aligns with the Hoogsteen edge of the acceptor, such as in G•G•G•G tetrads and sheared G•A mismatches, respectively. Examples are demonstrated on the following uniformly ^{15}N,^{13}C-labelled systems: (a) an RNA regulatory element involving the HIV-1 TAR RNA fragment (Figure 2a), (b) a multi-stranded DNA architecture involving a G•(C-A) triad-containing G-quadruplex (Figure 3a) (Kettani et al., 2000b) and (c) a peptide-RNA complex involving an evolved peptide bound to the HIV-1 Rev response element (RRE) RNA fragment (Figure 2b) (Gosser et al., 2001).

NMR spectroscopy

The magnetization transfer schemes and details of pulse sequences for the *trans*-hydrogen bond ^{1}H-^{1}H correlation experiments are shown in Figure 4a–d. A product operator outline for each sequence is presented below, followed by a brief discussion,. All coupling constant information has been obtained from the review by Wijmenga and van Buuren (1998).

A–U correlations: the H2(N1N3)H3 sequence

This is the simplest of H(NN)H schemes, which also illustrates some of the general principles used in all the pulse sequences described here. Magnetization transfer proceeds in the direction: H2(A, t_1) → N1(A) → N3(U) → H3(U, t_2). A product operator outline is as follows:

$$H2_y(t_1) \xrightarrow{^{2}J_{H2N1}} 2H2_xN1_z \xrightarrow{90^{y}_{H},\,90^{x}_{N}} 2H2_zN1_y$$
$$\xrightarrow{^{2}J_{H2N1},\,^{2h}J_{N1N3}} 2N1_yN3_z \xrightarrow{90^{x}_{N}} 2N1_zN3_y$$
$$\xrightarrow{^{2h}J_{N1N3},\,^{1}J_{H3N3}} 2N3_yH3_z \xrightarrow{90^{x}_{H},\,90^{x}_{N}} 2H3_yN3_z$$
$$\xrightarrow{^{1}J_{H3N3}} H3_x(t_2)$$

The sequence begins with the generation of transverse H2 magnetization of adenine, which evolves under the $^{2}J_{H2N1}$ coupling, during the constant time $2\times T_{nh}$ evolution period ($T_{nh} \sim$ 10–15 ms). To avoid the 'diagonal peak' pathway H3(U)/H1(G) (t_1) → N3(U)/N1(G) →H3(U)/H1(G) (t_2), a selective off-resonance inversion pulse is applied at the center of N3(U) and N1(G) with a null at N1, in the middle of the t_1 period. Proton magnetization is then transferred to the N1 nitrogen, which refocuses w.r.t. the $^{2h}J_{H2N1}$ coupling and evolves under the $^{2h}J_{N1N3}$ coupling during the subsequent $2\times t_{nn}$ period. Using a cosine modulated selective 180° pulse with simultaneous, selective excitation maxima at the N1 and N3 frequencies improves the sensitivity of the experiment considerably relative to that of a 'hard' (or composite) 180° pulse, which also engages undesirable scalar coupling pathways. To avoid Bloch–Siegert type phase shifts due to the simultaneous excitation, the duration of the pulse needs to be carefully adjusted, typically to multiples of $1/\delta_{N1N3}$ where δ_{N1N3} is the frequency difference between the centers of the N1(A) and N3(U) regions (Sklenár et al., 1999). At the end of the first $2\times t_{nn}$ period, coherence is transferred to the N3 nitrogen of uridine, which refocuses w.r.t. the $^{2h}J_{N1N3}$ coupling during the second $2\times t_{nn}$ period. Evolution under the $^{1}J_{N3H3}$ coupling occurs in the final $1/2J_{NH}$ (ε) period during which ^{1}H decoupling is terminated. In the final step, magnetization is transferred to the H3 proton for detection. In larger systems, increased sensitivity may be achieved by eliminating ^{1}H decoupling and using a TROSY based approach (Dingley and Grzesiek, 1998; Pervushin et al., 1997) for the N3 → H3 step. Throughout the sequence, water-flipback (Grzesiek and Bax, 1993) and watergate elements (Piotto et al., 1992) are used for optimal water-suppression. The 2D spectrum yields cross peaks between H2(ω_1) and H3 (ω_2) protons.

In principle, this sequence can also be acquired in reverse, that is, the transfer pathway can be H3(t_1) → N3 → N1 → H2(t_2). The sequence then becomes similar to that of the H_2(N2N7)H8 experiment described below.

G–C correlations: the H5(N3N1)H1 experiment

The H5(N3N1)H1 and H6(N3N1)H1 sequences constitute the H(CNN)H class of experiments. In the H5(N3N1)H1 sequence, magnetization transfer proceeds as: H5(t_1) → C5 → C4 → N3 → N1 →H1(t_2) (Figure 4b). The series of concatenated INEPT trans-

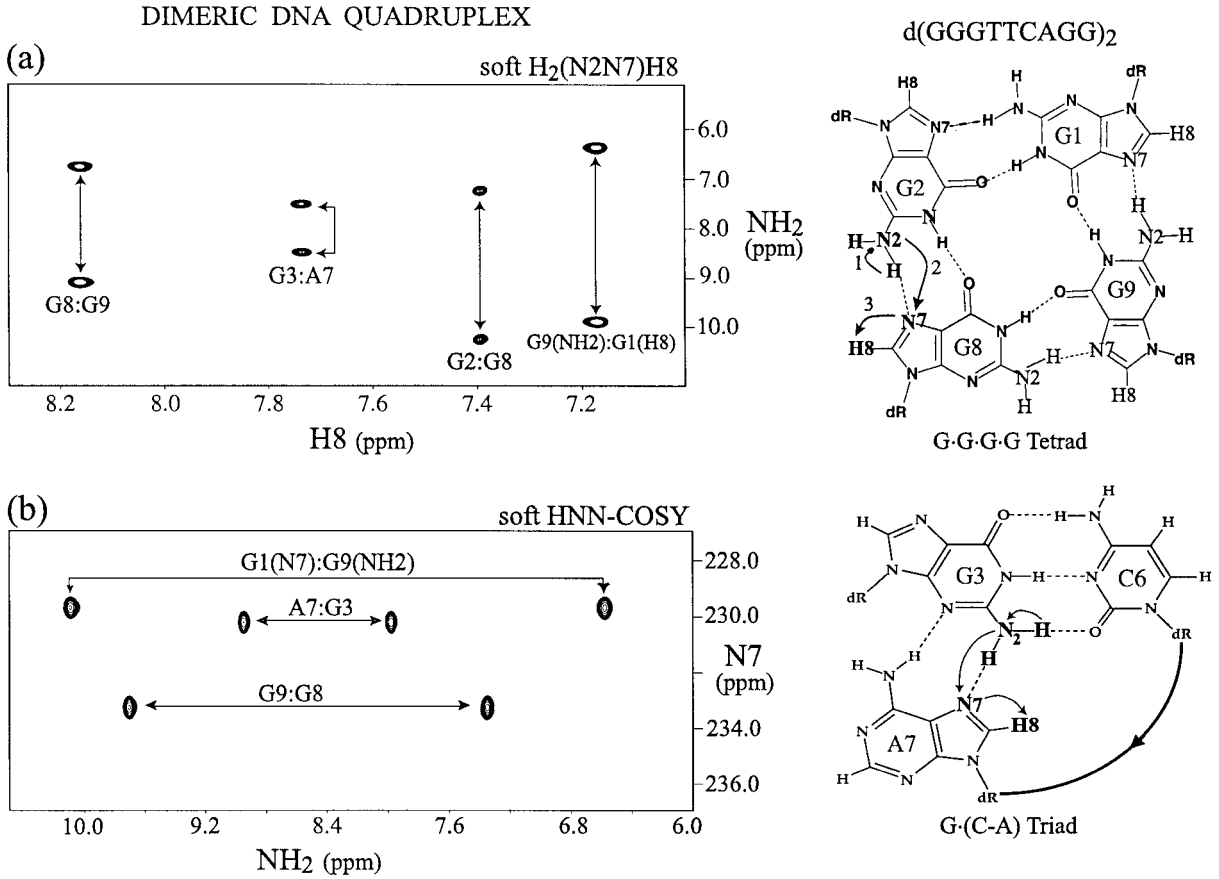

Figure 7. Regions of (a) soft H_2(N2N7)H8 and (b) soft HNN-COSY spectra of the uniformly $^{13}C/^{15}N$ labeled d(GGGTTCAGG) DNA fragment that forms a dimeric quadruplex, showing cross peaks between NH_2 protons of guanine (indicated with lines) and (a) H8 protons, and (b). N7 nitrogens of guanine/adenine. Schematics of the G•G•G•G tetrad and G•(C–A) triad motifs are also shown. Acquisition parameters were: number of transients: (a) 96, (b) 112; complex data points (ω_2, ω_1): (a) (576, 64), (b) (960, 80); spectral widths in kHz (ω_2, ω_1): (a) (4.8, 4.8), (b) (12.0, 2.0); resolution in ms (t_2^{max}, t_1^{max}): (a) (72,13), (b) (80, 39.5); relaxation delay (s): (a) 1.4, (b) 1.5; total data acquisition time (h): (a) 6.0, (b) 10.0. Adequate S/N was achieved in about half the total acquisition time. The H_2(N2N7)H8 spectrum was folded in the ω_1 dimension.

fers that achieve the desired transformation are as follows:

$$H5_y \xrightarrow{^1J_{C5H5}} 2H5_xC5_z(t_1) \xrightarrow{90^y_H,\ 90^x_C} 2H5_zC5_y$$

$$\xrightarrow{^1J_{H5C5},\ ^1J_{C4C5}} 2C5_yC4_z \xrightarrow{90^x_{C5},\ 90^x_{C4}} 2C5_zC4_y$$

$$\xrightarrow{^1J_{C5C4},\ ^1J_{C4N3}} 2C4_yN3_z \xrightarrow{90^x_C,\ 90^x_N} 2C4_zN3_y$$

$$\xrightarrow{^1J_{C4N3},\ ^{2h}J_{N3N1}} 2N3_yN1_z \xrightarrow{90^x_N} 2N3_zN1_y$$

$$\xrightarrow{^{2h}J_{N3N1},\ ^1J_{N1H1}} 2N1_yH1_z$$

$$\xrightarrow{90^x_N,\ 90^x_H} 2N1_zH1_y \xrightarrow{^1J_{N1H1}} H1_x(t_2)$$

Most elements are very similar to the H2(N1N3)H3 experiment and therefore, only key features will be described. A BIRD sequence (Bax, 1983) restores H_2O magnetization to equilibrium while simultaneously generating antiphase $H5_xC5_z$ magnetization. After frequency labeling of the H5 proton during the subsequent t_1 period, coherence is transferred to the C5 carbon. From the C5 carbon to the N3 nitrogen, the protocol closely follows that of Wöhnert et al. (1999b), for intraresidue correlations of H5 protons with exchangeable protons in cytosine and uridine bases. Since the chemical shifts of C5 and C4 are separated by about 67 ppm ($\sim$ 11 kHz at 14.1 T), efficient $^1J_{C5C4}$ evolution during the $2\times t_{cc}$ period requires a shaped pulse with simultaneous excitation points at C5 and C4 and a null at C6 to avoid $^1J_{C5C6}$ evolution, with the pulse duration adjusted to avoid phase distortions at the C5 frequency (Sklenár et al., 1999). Selec-

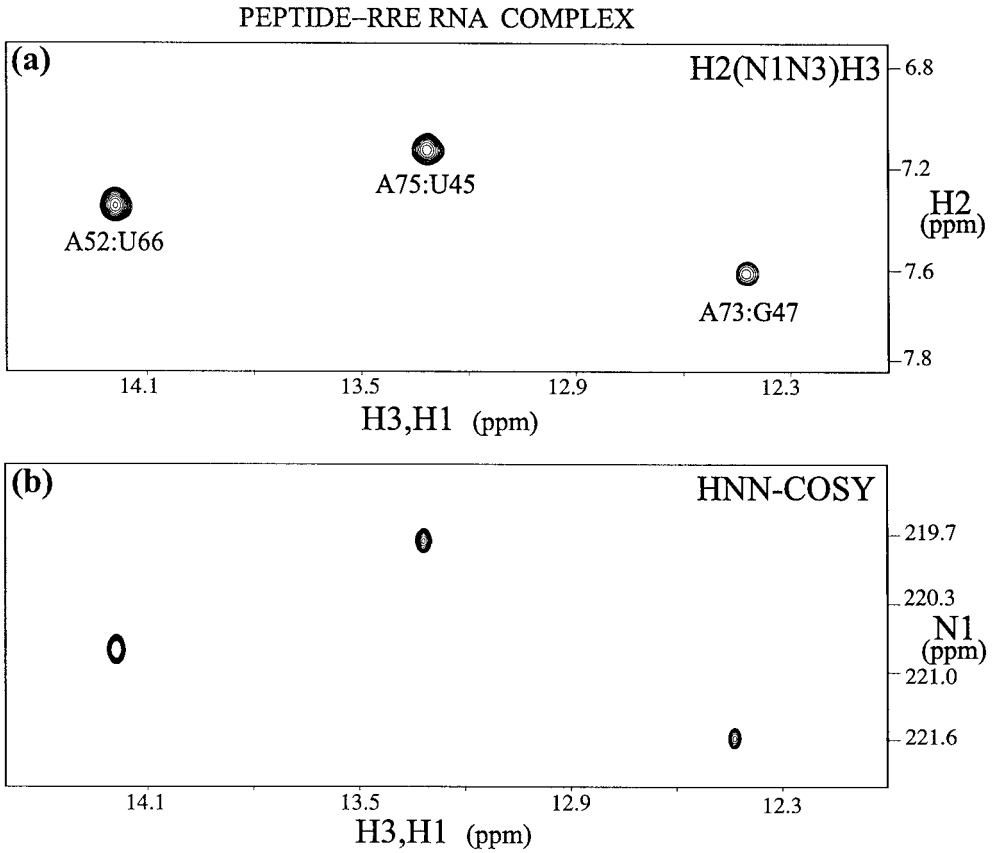

Figure 8. Regions of H2(N1N3)H3 (a) and HNN-COSY (b) spectra of the uniformly $^{13}C/^{15}N$ labeled RRE RNA-peptide (unlabeled) complex, in which uridine H3 protons involved in the two Watson–Crick A–U base pairs and a guanine H1 proton involved in a mismatched A•G base pair show cross peaks to (a) H2 protons and (b) N1 nitrogens of adenine. The sequence and folding topology of the RNA is shown in Figure 2b. The H2(N1N3)H3 spectrum was acquired with 32 transients, 2048 t_2 and 80 t_1 complex data points, spectral widths of 14.0 (ω_2) and 4.0 (ω_1) kHz, (t_2^{max} = 73 ms, t_1^{max} = 20 ms), and a relaxation delay of 1.5 s, resulting in total data acquisition time of ~2.5 h. The HNN-COSY spectrum was acquired with 32 transients, 1024 t_2 and 165 t_1 complex data points, spectral widths of 14.0 (ω_2) and 5.5 (ω_1) kHz, (t_2^{max} = 73 ms, t_1^{max} = 45 ms), and a relaxation delay of 1.5 s, resulting in total data acquisition time of 5.0 h. The apparent differences in line-widths between the spectra in (a) and (b), especially in the ^1H dimension, are primarily due to differences in window functions.

tive pulses are also required for efficient $C5_yC4_z \rightarrow C5_zC4_y$ transfer, as well as during the subsequent C4→N3 ($2\times t_{cn}$) period, for refocusing of the $^1J_{C5C4}$ coupling and evolution under the $^1J_{C4N3}$ (~7 Hz) coupling, especially because the small $^1J_{C4N3}$ coupling compares unfavorably with the larger, competing $^1J_{C4N4}$ (~20 Hz) coupling. The C4 → N3 step clearly represents the weakest link in the steps leading up to magnetization transfer to the N3 nitrogen. The N3(C) → N1(G) ($2\times t_{nn}$) step across the hydrogen-bond also requires selective inversion pulses on the C4 carbon to refocus the $^1J_{C4N3}$ coupling, and cosine modulated pulses with simultaneous N1(G)/N3(C) excitation, to avoid undesirable leakage via the $^1J_{N3C2}$ (~8 Hz) and $^2J_{N3N4}$ (~6 Hz) pathways, both of which compete strongly with the $^{2h}J_{N1N3}$ (5–6 Hz) coupling. After the $2\times t_{nn}$ period, coherence is transferred to the N1 nitrogen and finally, to the H1 proton for detection. The spectrum yields cross peaks between cytosine H5(ω_1) and guanine H1(ω_2) protons.

Needless to say, the sensitivity of this experiment is poorer than the H2(N1N3)H3 experiment, due to the larger number of transfer steps involved. The transfer from H5 to C4 is fairly efficient because of the large $^1J_{C5C4}$ coupling constant, but the small $^1J_{C4N3}$ coupling (~7 Hz) acts as a bottleneck in the transfer to the N3 nitrogen. However, careful usage of selective pulses to keep the magnetization transfer events focused on the desired pathway as well as to optimize excitation efficiency keeps the sensitivity of the sequence adequately high for moderately sized molecules. This sequence can also be designed for 'reverse'

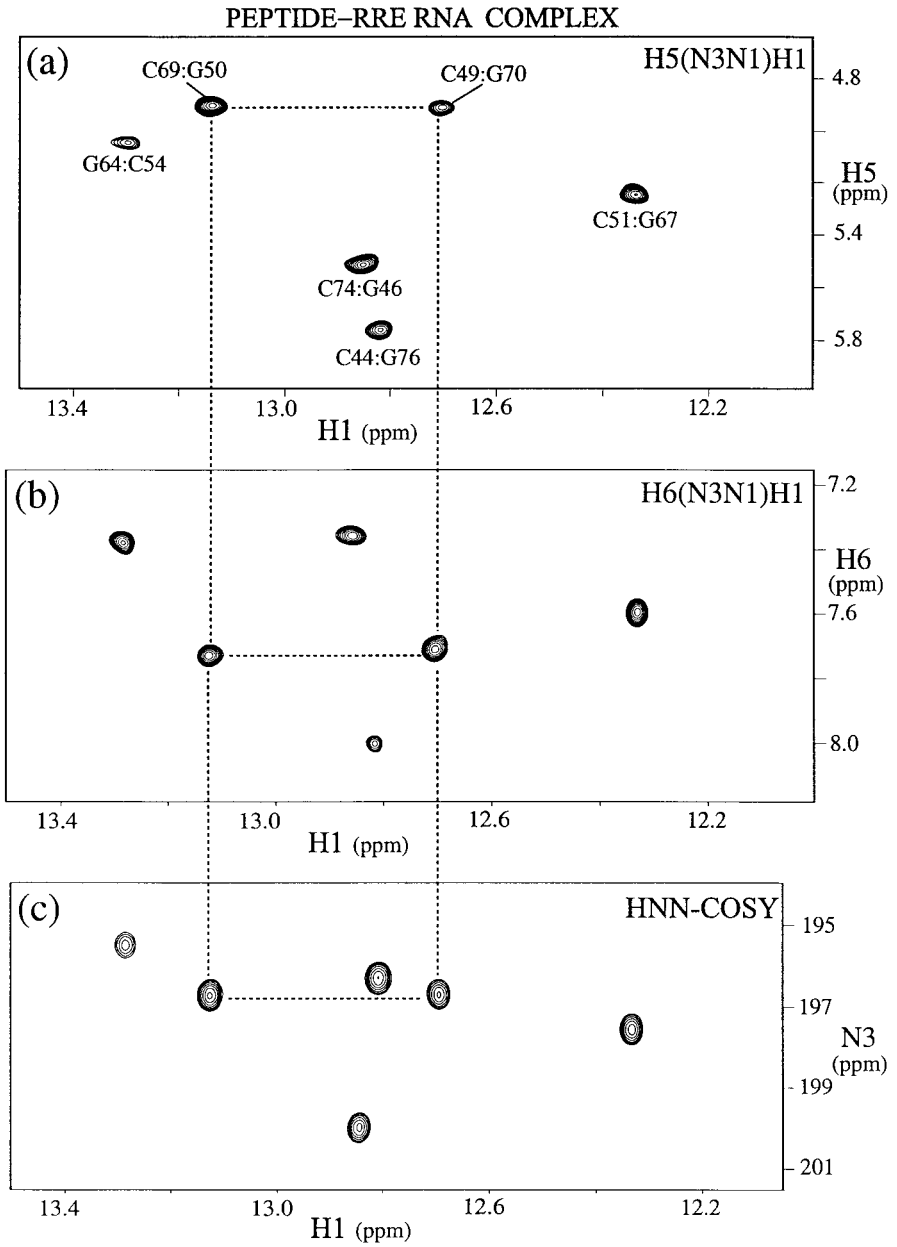

Figure 9. Regions of the (a) H5(N3N1)H1, (b) H6(N3N1)H1 and (c) HNN-COSY spectra of the uniformly $^{13}C/^{15}N$ labeled HIV RRE RNA-peptide complex, showing cross peaks between H1 protons of guanine and (a) H5 and, (b) H6 protons, and (c) N3 nitrogens of cytosine, in six of the seven Watson–Crick G–C base pairs (see Figure 2b). Dashed lines indicate the degeneracy of the G50:C69 and G70:C49 cross peaks in both the HNN-COSY as well as the H5(N3N1)H1 spectrum and its subsequent, although marginal, resolution in the H6(N3N1)H1 spectrum. Each spectrum was acquired with 1024 complex data points, a spectral width of 14 kHz along t_2(t_2^{max} = 73 ms), and a relaxation delay of 1.5 s. Other parameters were: number of transients: (a) 96, (b) 144, (c) 32; complex data points along t_1: (a) 72, (b) 36, (c) 165; spectral width along ω_1(kHz): (a) 1.8, (b) 1.8, (c) 5.5; t_1^{max} (ms): (a) 39, (b) 20, (c) 30; total data acquisition time (h): (a) 6.5, (b) 5.0, (c) 5.0. Adequate S/N was achieved in (a) and (b) in about half the total acquisition time. The H6(N3N1)H1 spectrum was folded in the ω_1 dimension.

operation ($H1(t_1) \rightarrow N1 \rightarrow N3 \rightarrow C4 \rightarrow C5 \rightarrow H5(t_2)$), but is not desirable since the H5 protons resonate very close to the water resonance thereby demanding extremely high quality water-suppression.

G–C correlations: the H6(N3N1)H1 experiment

In this companion H(CNN)H sequence, the H6 proton is frequency labeled during t_1, after which magnetization is transferred to the C6 carbon and then to C5 via a ^{13}C TOCSY (DIPSI-3, Shaka et al., 1988) sequence (Figure 4c):

$$H6_y \xrightarrow{^1J_{H6C6}} H6_xC6_z(t_1) \xrightarrow{90^y_H,\, 90^x_C} H6_zC6_y \xrightarrow{^1J_{H6C6}} C6_x \xrightarrow{90^y_C} C6_z \xrightarrow{^1J_{C6C5}} C5_z \xrightarrow{90^y_C} C5_x$$

All subsequent steps are identical to the H5(N3N1)H1 experiment described above and yields cross peaks between cytosine H6(ω_1) and guanine H1(ω_2) protons. This is clearly the least sensitive of the above series of experiments. However, since $^1J_{C6C5}$ is about 68 Hz in cytosine, C6→C5 transfer is quantitative in about 7.5 ms, which does not affect the sensitivity seriously. Since H5→C5 transfer is also active simultaneously, both C6 and C5 magnetization is present prior to the TOCSY period. As a result, by varying the mixing time appropriately, simultaneous H6(ω_1),H1(ω_2) and H5(ω_1),H1(ω_2) correlations may be obtained in the same spectrum, albeit with a reduction in overall sensitivity.

Mismatches: the soft H_2(N2N7)H8 experiment

This sequence (Figure 4d) is essentially the reverse of the H(NN)H experiment described above for H2(A):H3(U) correlations, with additional incorporation of selective pulses to achieve magnetization transfer between N2 and N7 nitrogens which have very well-separated chemical shifts ($\delta_{N2N7} \sim 160$ ppm). In principle, this sequence can be readily applied to any coupling topology of the form N_d–H_d•••$N_a \rightarrow H_a$ (d = donor, a = acceptor), where $N_a \rightarrow H_a$ represents a long range $^mJ_{NaHa}$ ($m > 1$) coupling . Here, we specifically consider NH_2•••N7→H8 topologies that exist in several commonly occurring mismatches (see Introduction). Magnetization transfer proceeds as $H_2(t_1) \rightarrow N2 \rightarrow N7 \rightarrow H8\ (t_2)$. The product operator outline of the sequence is as follows:

$$(H2_{1y} + H2_{2y})(t_1) \xrightarrow{^1J_{NH}} (2H2_{1x}N2_z + 2H2_{2x}N2_z) \xrightarrow{90^y_H,\, 90^x_N} (2H2_{1z}N2_y + 2H2_{2z}N2_y) \xrightarrow{^1J_{NH},\, ^{2h}J_{N2N7}} 2N2_yN7_z \xrightarrow{90^x_{N2},\, 90^x_{N7}} 2N2_zN7_y \xrightarrow{^{2h}J_{N2N7},\, ^2J_{N7H8}} 2N7_yH8_z \xrightarrow{90^x_N,\, 90^x_H} 2H8_yN7_z \xrightarrow{^2J_{N7H8}} H8_x(t_2)$$

Magnetization originates on the amino protons and is transferred to the amino nitrogen via an INEPT element. For exchange broadened amino protons, the sequence may be easily modified to replace the INEPT transfer with an appropriate CPMG sequence (Gullion et al., 1990; Mueller et al., 1995). After transfer to the amino nitrogen, evolution under the $^{2h}J_{N2N7}$ coupling takes place for a period $2\times t_{nn}$ during which the $^1J_{NH}$ coupling is refocused using ^1H decoupling after a time $1/4J_{NH}$ (ε). Since amino and N7 nitrogen frequencies are widely separated (∼ 150–160 ppm), selective 180° and 90° pulses are used for the N2→N7 transfer steps, as described previously (Majumdar et al., 1999a,b; Dingley et al., 2000). The N7 magnetization then evolves under the $^2J_{N7H8}$ (∼ 11 Hz) coupling during $2\times T_{nh}$ and is transferred to the H8 proton for detection. The spectrum consists of cross peaks between the two NH_2 protons (ω_1) and the H8 proton (ω_2). If the chemical shift separation between the donor and acceptor nitrogens is not significant, hard pulses may be used to achieve the $N_d \rightarrow N_a$ transfer which is essentially the reverse of the H2(N3N1)H3 sequence. In our experience, the relative sensitivity of the two sequences is dictated largely by the system under study, based on the interplay of relaxation and exchange broadening effects.

Materials and methods

All spectra were recorded on Varian INOVA spectrometers operating at 14.1 T (600 MHz, ^1H frequency), equipped with actively shielded z-gradient probes. To demonstrate the H2(N1N3)H3, H5(N3N1)H1 and H6(N3N1)H1 experiments, the following uniformly $^{13}C/^{15}N$ labeled samples were prepared using standard procedures described previously (Cai et al., 1998): (a) A 27 nucleotide fragment of HIV-1 TAR RNA

(mol. wt. ~9 kD) in 95% H_2O/5% D_2O solution containing 15 mM phosphate/25 mM Na_2SO_4/0.1 mM EDTA buffer at pH 6.1 and 25 °C; (b) a 31-nucleotide fragment derived from stem IIB of the HIV-1 Rev response element (RRE) mRNA, complexed with an (unlabeled) 22 residue peptide (mol. wt. ~13 kD) (Gosser et al., 2001), in 95% H_2O/5% D_2O solution containing 10 mM phosphate/12.5 mM NaAc-d_4 buffer, at pH 6.0 and 25 °C. To demonstrate the NH_2(N7)H8 experiment, a dimeric DNA quadruplex, d($G_1G_2G_3T_4T_5C_6A_7G_8G_9$) (mol. wt. ~6 kD) (Kettani et al., 2000b) was uniformly $^{13}C/^{15}N$ labeled using the procedure described in Kettani et al. (1999), in 95% H_2O/5% D_2O solution, containing 100 mM NaCl/2 mM phosphate buffer, at pH 6.5 and 0 °C. All sample concentrations were approximately 1.5 mM.

Results

Watson–Crick base pairs: HIV-1 TAR RNA

Protein-RNA recognition plays a key role in the life cycle of lentiviruses. Transcription of the integrated provirus is stimulated by a *trans* activating protein Tat through interaction with the *trans* activation response (TAR) element of the transcribed mRNA (reviewed in Karn, 1999). The sequence of HIV-1 TAR shown in Figure 2a contains an internal three base bulge, which is the target site for the Tat protein. Our laboratory is interested in the interaction of HIV-1 TAR with small molecules capable of disruption of the Tat-TAR complex. To this end, we are applying hydrogen bonding and residual dipolar coupling methodologies in our laboratory to supplement earlier available NOE data (Puglisi et al., 1993; Aboul-ela et al., 1995; Brodsky & Williamson, 1997) for structure determination of the HIV-1 TAR in the free and bound states.

Figure 5a shows a region of the H2(N1N3)H3 spectrum recorded on the HIV-1 TAR RNA fragment, consisting of cross peaks between the H2 protons of A20 and A27 and the imino (H3) protons of their base paired partners, U42 and U38, respectively. Evidence for the A22–U40 base pair could not be obtained either by HNN-COSY methods (due to exchange broadening of the H3 proton of U40) or H(CN)N(H) techniques to correlate H2:A22 with N3:U40. The HNN-COSY spectrum correlating the uridine H3 protons with adenine N1 nitrogens is shown in Figure 5b. Figure 5a clearly demonstrates the feasibility of obtaining ^{1}H-^{1}H correlations across A–U base pairs, thereby eliminating the need for separately assigning the N1 nitrogen. In systems with substantial degeneracy in the N1 region, these correlations can be significantly useful in circumventing N1 overlap problems.

This aspect becomes evident in Figures 6a–c showing G–C correlation spectra of the TAR fragment. The H5(N3N1)H1 spectrum (Figure 6a) shows H5(C,ω_1):H1(G,ω_2) cross peaks; the H6(N3N1)H1 spectrum (Figure 6b) shows corresponding H6(C,ω_1): H1(G,ω_2) correlations, and N3(C,ω_1):H1(G,ω_2) correlations are observed in the HNN-COSY spectrum (Figure 6c). All cross peaks are observed, barring the terminal G–C pair where the imino proton is too exchange broadened to be observable. For the TAR fragment, it is clear that the H5(N3N1)H1 spectrum not only eliminates the need for independent assignment of the cytosine N3 nitrogen, but also removes the degeneracy associated with these nitrogens – notably C41, C44 and C37 – in the HNN-COSY spectrum of Figure 6c. The H6(N3N1)H1 spectrum in Figure 6b turns out to be less useful for TAR because the H6 protons are not as well dispersed as the H5 protons. However, as discussed below for the RRE-peptide complex, situations may arise where the H6(N3N1)H1 spectrum may play a critical role. In any case, convergent information obtained from complementary data sets is always beneficial.

Mismatch alignments: multi-stranded, higher-order DNA architecture

Our laboratory has been interested in defining the folding topology of higher order multi-stranded DNA architectures stabilized through mismatch, triple, triad, tetrad and hexad alignments (reviewed in Patel et al., 1999). The identification of pairing alignments constitutes a key process in differentiation amongst alternate folding topologies and this is achievable through identification of donor and acceptor pairs within individual hydrogen bond pairing alignments. Such an approach has been used in our laboratory on a variety of novel multi-stranded folding topologies recently ranging from mismatch-aligned duplexes (Kettani et al., 1999), to dimeric quadruplexes containing stacked triads (Figure 2a) (Kettani et al., 2000b), and four-stranded quadruplexes stabilized through hexad formation (Kettani et al., 2000a).

Figure 7a shows the soft H_2(N2N7)H8 spectrum recorded on d(GGGTTCAGG), which forms a dimeric G(C•A) containing quadruplex (Figure 3a) (Kettani et al., 2000b), showing $NH_2(\omega_1)$:H8(ω_2) cross peaks

mediated via $^{2h}J_{N2N7}$ coupling constants across G•G mismatches in the G•G•G•G tetrad and the sheared G•A mismatch in the G•(C-A) triad. Figure 7b shows the corresponding soft-HNN COSY spectrum showing N7(G/A,ω_1):N2H$_2$(G,ω_2) cross peaks. Possible ambiguities arising from the near degeneracy of the N7 nitrogens of G1 and A7 are immediately resolved in the soft H$_2$(N2N7)H8 spectrum due to the clear separation of the H8 protons. This is achieved despite the substantially lower intrinsic resolution of the H$_2$(N2N7)H8 spectrum along ω_1 ($t_1^{max} = 13$ ms) relative to the soft HNN COSY spectrum (~ 40 ms). In addition, the N7(G8,ω_1):NH$_2$(G2,ω_2) correlation, which is missing from the soft HNN COSY experiment is observable as a NH$_2$(G8,ω_1):H8(G2,ω_2) cross peak in the soft H$_2$(N2N7)H8 spectrum. The exchange broadened NH$_2$ protons of G2 are observed as weak peaks in the ^{1}H-^{15}N HSQC spectrum, but do not survive the longer delays contained in the soft HNN COSY sequence. However, in the H$_2$(N2N7)H8 sequence, detection on non-exchangeable H8 protons permits observation of this correlation. The only cross peak missing from both spectra is the G2:G1 correlation, because the G2:NH$_2$ protons are too severely exchange broadened and not observable even in the ^{1}H-^{15}N HSQC.

RNA-peptide complexes: evolved peptide-RRE complex

Recently, progress has been made towards the structural characterization of complexes between arginine-rich peptides and their RNA targets in viral and phage systems (reviewed in Patel, 1999; Frankel, 2000). Such studies have the advantage that the peptide and RNA components are minimalist modular domains capable of undergoing adaptive structural transitions on complex formation. Minimalist elements of protein secondary structure are enveloped within major groove binding pockets within the RNA, with recognition involving intermolecular interactions between peptide backbone and side chains and precisely positioned mismatches, triples and looped out bases of the RNA pocket. Recent structural studies from our laboratory of two distinct peptides binding the same RNA, has established that RNA defines the conformation of the bound peptide (Ye et al., 1999). Conversely, studies from our laboratory of one peptide binding two distinct RNAs, has established a peptide-triggered conformational switch in HIV-1 RRE RNA complexes (Gosser et al., 2001). In the latter study, we investigated the NMR structure of the high affinity complex between an evolved peptide (Harada et al., 1997) and the RRE target (Gosser et al., 2001).

Figures 8 and 9 show H2(N1N3)H3, H5(N3N1)H1, H6(N3N1)H1 and HNN-COSY spectra recorded on the evolved-peptide RRE complex. Figures 8a and 8b show regions of the H2(N1N3)H3 and HNN-COSY spectra, respectively. Note that the H2(N1N3)H3 spectrum successfully reports the H2(A,ω_1):H3(G,ω_2) correlation for an A•G mismatch, in addition to the A–U Watson–Crick base pairs. Figures 9a–c show regions of the H5(N3N1)H1, H6(N3N1)H1 and HNN-COSY spectra, respectively, on the same system, highlighting correlations across G–C Watson–Crick base pairs. It must be noted here that the ^{1}H-^{1}H correlation experiments were performed using less sensitive, 'first-generation' versions of the sequences presented here and therefore required significantly longer acquisition times than the newer versions that have been used in Figures 5–7. Even so, these spectra demonstrate the high quality of data that may be obtained on larger, complex systems (~ 13 kD). Figure 9 also points out an important application of the H6(N3N1)H1 spectrum: in the peptide-RRE complex, the degeneracy of the N3 nitrogens of cytosines 49 and 69 in the HNN-COSY spectrum (Figure 9c) is *not* lifted by the H5(N3N1)H1 experiment (Figure 9a), since the H5 protons are also degenerate! It is in the H6(N3N1)H1 spectrum (Figure 9b) that the corresponding H6 protons resolve the degeneracy, although by a narrow margin. This illustrates the complementary nature of the H5(N3N1)H1 and H6(N3N1)H1 experiments.

Discussion

In this paper we have presented novel methods H(NNH) and H(CNN)H based methods for correlating exchangeable protons with non-exchangeable protons across N-H• • •N hydrogen bonds, under conditions where exchangeable protons are detectable. These ^{1}H-^{1}H correlation experiments complement the HNN-COSY technique effectively by eliminating the need for assigning the donor/acceptor nitrogen, and thereby circumventing problems of degeneracy in the nitrogen dimension. There are other possible applications of these experiments as well, such as in the resonance assignment procedure. These techniques may also be extended to the detection of ^{1}H-^{1}H correlations across *inter*-molecular N–H•••N hydrogen bonds to comple-

ment the HNN-COSY and H(CN)N(H) methods used previously (Liu et al., 2000b).

The ^{1}H-^{1}H correlation experiments can be conveniently augmented by equivalent ^{1}H-^{13}C correlations. A simple approach is to replace the frequency labeling of the non-exchangeable proton in the indirect dimension with that of the directly bonded carbon, i.e., the H2(N1N3)H3, H5(N3N1)H1 and H6(N3N1)H1 sequences may be substituted by corresponding C2(N1N3)H3, C5(N3N1)H1 and C6(N3N1)H1 sequences, respectively, with minor modifications to the experimental protocols described here. The two approaches may also be combined to yield appropriate $H_aC_a(N_bN_c)H_d$ type of 3D spectra as well.

With regard to sensitivity, the experiments performed quite well on the systems and sample conditions used in this study. The least sensitive of the pulse-sequences, namely, the H6(N3N1)H1 experiment, demonstrated adequate S/N within 2–3 h of data acquisition, even with a non-optimized version of the sequence, on the largest system – the 13 kD peptide-RRE complex – used in this work. It must be borne in mind that these sequences are sensitive to the choice of selective pulses in terms of focusing the magnetization transfer along the desired pathway, and efficient excitation of well-separated nuclei. Also, since one of the protons correlated by these experiments is always an exchangeable proton, exchange broadening effects are bound to degrade sensitivity. We anticipate that these experiments will be adequately sensitive for moderately sized systems ($\sim$15 kD) and may be extendable to larger molecules under favorable relaxation and exchange broadening conditions. In conjunction with relaxation optimized techniques such as TROSY (Pervushin et al., 1997; Pervushin, 2001), we hope to extend the domain of applicability to even larger molecules.

Acknowledgements

This work was supported under grant no. GM34504, GM54777 and CA49982 to DJP. We thank Natalya Chernichenko, Eugene Skripkin and Weijun Xu for preparation and purification of ^{13}C/^{15}N-labeled RNA and DNA oligomers.

References

Aboud-ela, F., Karn, J. and Varani, G. (1995) *J. Mol. Biol.*, **253**, 313–332.

Al-Hashimi, H.M., Majumdar, A., Gorin, A., Kettani, A., Skripkin, E. and Patel, D. J. (2001a) *J. Am. Chem. Soc.*, **123**, 633–640.

Al-Hashimi, H.M., Gorin, A., Majumdar, A. and Patel, D.J. (2001b) *J. Am. Chem. Soc.*, **123**, 3179–3180.

Barfield, M., Dingley, A.J., Feigon, J. and Grzesiek, S. (2001) *J. Am. Chem. Soc.*, **123**, 4014–4022.

Bax, A. (1983) *J. Magn. Reson.*, **53**, 517–520.

Brodsky, A.S. and Williamson, J.R. (1997) *J. Mol. Biol.*, **267**, 624–639.

Cai, Z., Gorin, A., Frederick R., Ye, X., Hu, W., Majumdar, A., Kettani, A. and Patel, D.J. (1998) *Nat. Struct. Biol.*, **5**, 203–212.

Dingley, A.J. and Grzesiek, S. (1998) *J. Am. Chem. Soc.*, **120**, 8293–8297.

Dingley, A.J., Cordier, F. and Grzesiek, S. (2001) *Concepts Magn. Reson.*, **13**, 103–127.

Dingley, A.J., Masse, J.E., Feigon, J. and Grzesiek, S. (2000) *J. Biomol. NMR*, **16**, 279–289.

Dingley, A.J., Masse, J.E., Peterson, R.D., Barfield, M., Feigon, J. and Grzesiek, S. (1999) *J. Am. Chem. Soc.*, **121**, 6019–6027.

Emsley, L. and Bodenhausen, G. (1990) *Chem. Phys. Lett.*, **165**, 469–476.

Frankel, A.D. (2000) *Curr. Opin. Struct. Biol.* **10**, 332–340.

Gemmecker, G. (2000) *Angew. Chem. Int. Ed. Engl.*, **39**, 1224–1226.

Gosser, Y., Hermann, T., Majumdar, A., Hu, W., Frederick, R., Jiang, F., Xu W. and Patel, D.J. (2001) *Nat. Struct. Biol.*, **8**, 146–150.

Grzesiek, S. and Bax, A. (1993) *J. Am. Chem. Soc.*, **115**, 12593–12594.

Grzesiek, S., Cordier, F. and Dingley, A.J. (2001) *Meth. Enzymol.*, **338**, 111–133.

Gullion, T., Baker, D.B. and Conradi, M.S. (1990) *J. Magn. Reson.*, **89**, 479.

Harada, K., Martin, S. S., Tan, R. and Frankel, A. D. (1997) *Proc. Natl. Acad. Sci. USA*, **94**, 11887–11892.

Hennig, M. and Williamson, J.R. (2000) *Nucl. Acids Res.*, **28**, 1585–1593.

Hermann, T. and Westhof, E. (1999) *Chem. Biol.*, **6**, 335–343.

Jiang, L., Majumdar, A., Hu, W., Jaishree, T.J., Xu, W. and Patel, D. J. (1999) *Structure*, **7**, 817–827.

Karn, J. (1999) *J. Mol. Biol.*, **293**, 235–254.

Kettani, A., Bouaziz, S., Skripkin, E., Majumdar, A., Wang, W., Jones, R.A. and Patel, D. J. (1999) *Structure*, **7**, 803–815.

Kettani, A., Gorin, A., Majumdar, A., Hermann, T., Skripkin, E., Zhao, H. and Jones R. (2000a) *J. Mol. Biol.*, **297**, 627–644.

Kettani, A., Basu, G., Gorin, A., Majumdar, A., Skripkin, E. and Patel, D. J. (2000b) *J. Mol. Biol.*, **301**, 129–146.

Kojima, C., Ono, A. and Kainosho, M. (2000) *J. Biomol. NMR*, **18**, 269–277.

Liu, A., Majumdar, A., Hu, W., Kettani, A., Skripkin E. and Patel, D. J. (2000a) *J. Am. Chem. Soc.*, **122**, 3206–3210.

Liu, A., Majumdar, A., Jiang, F., Chernichenko, N., Skripkin, E. and Patel, D.J. (2000b) *J. Am. Chem. Soc.*, **122**, 11226–1127.

Luy, B. and Marino, J. (2000) *J. Am. Chem. Soc.*, **122**, 8095–8096.

Majumdar, A., Kettani, A. and Skripkin, E. (1999a) *J. Biomol. NMR*, **14**, 67–70.

Majumdar, A., Kettani, A. and Skripkin, E. and Patel, D. J. (1999b) *J. Biomol. NMR*, **15**, 207–211.

Majumdar, A., Kettani, A., Skripkin, E. and Patel, D.J. (2001) *J. Biomol. NMR*, **19**, 103–113.

Marion, D., Ikura, M., Tschudin, R. and Bax, A. (1989) *J. Magn. Reson.*, **85**, 393–399.

Masquida, B. and Westhof, E. (2000) *RNA*, **6**, 9–15.

Mollova, E.T. and Pardi, A. (2000) *Curr. Opin. Struct. Biol.*, **10**, 298–302.

Mueller, L., Legault, P. and Pardi, A. (1995) *J. Am. Chem. Soc.*, **117**, 11043–11048.

Patel, D.J., Bouaziz, S., Kettani, A. and Wang, Y. (1999) In *Oxford Handbook of Nucleic Acid Structure*, Neidle, S. (Ed.), Oxford University Press, Oxford, pp. 389–453.

Pervushin, K. (2001) *J. Biomol. NMR*, **20**, 275–285.

Pervushin, K., Ono, A., Fernandez, A., Szyperski, T., Kainosho, M. and Wüthrich, K. (1998) *Proc. Natl. Acad. Sci. USA*, **95**, 14147–14151.

Pervushin, K., Riek, R., Wider, G. and Wüthrich, K. (1997) *Proc. Natl. Acad. Sci. USA*, **94**, 12366–12371.

Piotto, M., Saudek, V. and Sklenár, V. (1992) *J. Biomol. NMR*, **2**, 661–665.

Puglisi, J.D., Chen, L., Frankel, A.D. and Williamson, J.R. (1993) *Proc. Natl. Acad. Sci. USA*, **90**, 3680–3684.

Rudisser, S., Pelton, J.G. and Tinoco, I. (1999) *J. Biomol. NMR*, **15**, 173–176.

Shaka, A.J., Keeler, J. and Freeman, R. (1983) *J. Magn. Reson.*, **52**, 335–338.

Shaka, A.J., Lee, C.J. and Pines, A. (1988) *J. Magn. Reson.*, **77**, 274–293.

Sklenar, V., Masse, J.E. and Feigon, J. (1999) *J. Magn. Reson.*, **137**, 345–349.

Vuister, G.W. and Bax, A. (1992) *J. Magn. Reson.*, **98**, 428–435.

Westhof, E. and Fritsch, V. (2000) *Structure Fold Des.*, **8**, 55–65.

Wijmenga, S.S. and van Buuren, B.N.M. (1998) *Prog. NMR Spectr.*, **32**, 287–387.

Wöhnert, J., Dingley, A.J., Stoldt, M., Görlach, M., Grzesiek S. and Brown, L.R. (1999a) *Nucl. Acids Res.*, **27**, 3104–3110.

Wöhnert, J, Ramachandran, R., Görlach, M. and Brown, L.R. (1999b) *J. Magn. Reson.*, **139**, 430–433.

Ye, X., Gorin, A., Frederick, R., Hu, W., Majumdar, A., Xu, W., McLendon, G., Ellington, A. and Patel, D. J. (1999) *Chem. Biol.* **6**, 657–669.

Zidek, L.V., Stefl, R. and Sklenár, V. V. (2001) *Curr. Opin. Struct. Biol.*, **11**, 275–281.